Ignoring Dependence between Failure Modes is Reasonable for Low Probabilities of Failure

Chan Y. Park[1] Nam H. Kim[2], and Raphael T. Haftka[3]
University of Florida, Gainesville, FL, 32611-6250

For evaluating system reliability, dependence between failure modes has been usually ignored since it simplifies system reliability calculations. Interestingly, error due to ignoring dependence can be small when system reliability is high. There are three major factors affecting error: the strength of tail dependence, the magnitude of system reliability and the ratio between individual failure modes. We found that the error in system probability of failure (PF) due to ignoring dependence is small when system PF is small and tail dependence is not very strong or the ratio between contributions of individual failure modes is large. However, when system PF is small, even when errors due to tail dependence are substantial they are still comparable to unavoidable errors due to uncertainty in input distributions. With two dependent failure modes defined with the bivariate normal distribution, error in system reliability index becomes 1% for system reliability index of 3.28 and error in system PF becomes as low as 10% when system PF is less than 1.4×10-4 even with a strong dependence between failure modes, measured by a linear correlation coefficient of 0.8. For very strong tail dependence, error in system PF is as much as 70% when system PF is 10-5 but the error is comparable to error in such small system PF calculation from the other unavoidable error sources: errors in distributions for calculating PF. With a two bar truss example, sampling errors in ultimate strength distributions incurs more than 100% error for PF of 10-5 that is comparable to 70% due to ignoring strong tail dependence. A reliability-based optimization problem of a truss is also presented to show the effect of error on the optimum design.

I. Introduction

EVALUATING system reliability has been recognized as an important step in design. Although many reliability analysis methods have been developed, calculating system reliability including dependence between failure modes is still challenging [1].

Reliability analysis methods can largely be categorized by sampling-based methods (e.g., Monte Carlo Simulation (MCS), importance sampling and surrogate-based methods) and analytical methods (e.g., first-order reliability method (FORM) and second-order reliability method (SORM)).

MCS is a universal method, but it can be computationally expensive to achieve a reasonable accuracy, even when using importance sampling techniques to reduce the variance of MCS [2,3,4]. To evaluate reliability, surrogate-based methods have been developed to reduce computational cost [5]. Sampling-based methods using surrogates consider dependence between failure modes, but the computational cost of constructing surrogate models increases rapidly with dimension, often called the curse of dimensionality [6].

Analytical methods are computationally efficient for calculating reliability [4,7]. However, they have difficulties accounting for dependence between failure modes. Consequently, approximate approaches, such as the lower-upper bound method [7,8,9] and PNET method [10], have been developed.

However, it is not well known that dependence between failure events is usually weak for low PF [11]. Often structures are required to be highly reliable [13]. For example, the U.S. Army structural fatigue reliability criterion for rotorcraft has been interpreted as a requirement for component lifetime reliability of 0.999999 [14]. With such a high reliability, failures are extremely rare events. For such rare events, dependence between failure modes often becomes weak.

---

[1] Graduate Research Assistant, AIAA Student Member.
[2] Distinguished Professor, AIAA Fellow.
[3] Associate Professor, AIAA Member.

Ignoring dependence between input uncertainties can result in large errors in calculating system reliability [2]. Consequently modeling and identifying dependence between input model uncertainty is an important issue [15,16]. However, surprisingly, ignoring dependence between failure modes, which is recognizable as dependence between output uncertainties, may not result in large errors in system reliability.

The objectives of this paper are 1) to demonstrate that the error due to ignoring dependence on system reliability can be small even with strong dependence between failure modes, 2) to explore conditions where even for high reliability, the error may not be small and 3) to determine the significance of the error by comparing it to the errors in input distributions..

II. Dependence between Failure Modes and System Probability of Failure

Structural failure with multiple failure modes is modeled with uncertainties in limit states, which are also called output uncertainties. Dependence between failure modes is equivalent to dependence between output uncertainties. If there is a system with N failure modes, limit states are defined such that the ith failure event occurs when

$$G_i \le 0, \quad i=1,\ldots,\mathrm{N} \tag{1}$$

while the system is intact when

$$G_i > 0 \tag{2}$$

The PF of a single failure mode is referred to as a marginal PF that is defined as

$$P_{fi} = \Pr\left(G_i \le 0\right) \tag{3}$$

Two commonly used concepts for multiple failure modes are a series and parallel failure models. For the series failure model, the system fails if any of its failure modes is activated. For the parallel model, the system fails if all of its failure modes are activated [7]. The series failure model takes account of union of failures, and the parallel model takes account of intersection of failures. Both models are affected by dependence of failure modes. In this paper, the effect of ignoring dependence is discussed with the series model, since it is a common failure scenario in structural design.

A series model composed of two failure modes are defined using two limit states. System PF with dependent two failure modes (or exact system PF) is expressed as

$$P_{f,sys} = \Pr\left(\left\{G_1 \le 0\right\} \cup \left\{G_2 \le 0\right\}\right) \tag{4}$$

Using the well-known expansion theorem [8], the probability of the union of two events is decomposed as

$$P_{f,sys} = \Pr\left(G_1 \le 0\right) + \Pr\left(G_2 \le 0\right) - \Pr\left(\left\{G_1 \le 0\right\} \cap \left\{G_2 \le 0\right\}\right) \tag{5}$$

Approximate analytical methods have been developed to evaluate the system PF without integrating the joint PDF over the failure region [8,9,12]. However, if the error is not significant, assuming independence is more attractive since it makes the problem simple without any specialized methods. With the independence assumption, the system PF can be calculated based on the marginal PFs and the probability of the intersection with the independence assumption is expressed with Eq. (5) and

$$P_{f,sys}^{idp} = \Pr\left(G_1 \le 0\right) + \Pr\left(G_2 \le 0\right) - \Pr\left(G_1 \le 0\right)\Pr\left(G_2 \le 0\right) \tag{6}$$

where the superscript 'idp' represents the independence assumption.

A. Illustrative Truss Example

A simple two-member truss under a horizontal force *h* and vertical force *v* shown in Fig. 1 illustrates the dependence between limit states. The truss has two stress failure modes : failure of elements 1 and 2 when the corresponding stresses exceed the ultimate stress, σ_{u1}, that the material can sustain.

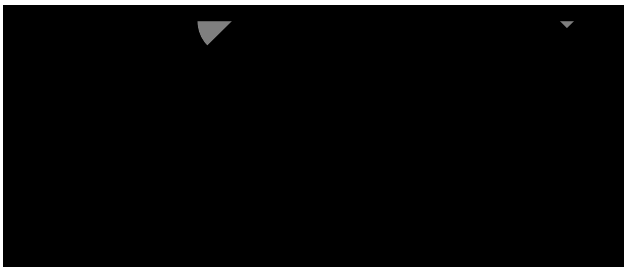

Figure 1: A simple truss example in biaxial loading

The limit state and the member force of element 1 are defined as

$$G_1 = A_1\sigma_{u1} - F_1$$
$$F_1 = \frac{1}{2}\left(\frac{v}{\cos\alpha} + \frac{h}{\sin\alpha}\right) \tag{7}$$

The limit state and the member force of element 2 are defined as

$$G_2 = A_2\sigma_{u2} - F_2$$
$$F_2 = \frac{1}{2}\left(\frac{v}{\cos\alpha} - \frac{h}{\sin\alpha}\right) \tag{8}$$

The ultimate strength and two external forces are input uncertainties, and the height of the structure and angle are deterministic. The values and distributions of these variables will be given in the reliability-based optimization example section.

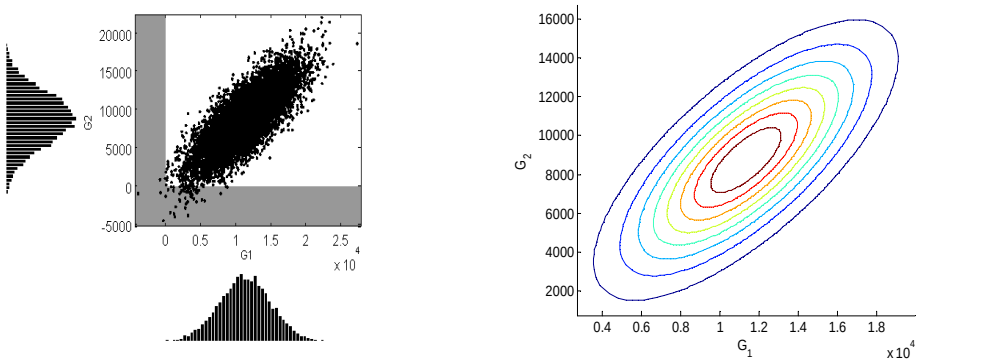

(a) Scatter plot of random samples (shaded region is the failure region)

(b) Contour plot of the joint PDF of G_1 and G_2

Figure 2: Scatter plot of two limit states

Figure 2(a) shows a scatter plot of 10,000 randomly generated limit state pairs, G_1 and G_2, which shows dependence between the two failure modes. The linear correlation coefficient between G_1 and G_2, is 0.79. Because the limit states are linear in the random variables and because these random variables are normally distributed, the joint probability density function (PDF) is bivariate Gaussian (normal). The system PF, P_{fsys}, is estimated as the ratio of the number of samples in the shaded area in Figure 2(a) to the total number of samples. The histograms shown on both axes are marginal histograms representing the marginal PDF of limit states. Figure 2(b) is a contour plot of the joint PDF of limit states G_1 and G_2, based on the 10,000 samples.

III. Error due to Ignoring Dependence on Evaluating System Reliability

A. Error due to Ignoring Dependence for Bivariate Gaussian Joint Distribution

It is easy to calculate the system PF if the two failure modes are assumed to be independent, but this incurs an error. Figure 3 shows the difference in intersection probability including and ignoring dependence between the two failure modes. Figure 3(a) shows 10,000 samples of the two dependent limit states. The samples are generated from the bivariate normal distribution with mean vector of (1.2,1.2) and the standard deviation vector of (1.0,1.0), and a correlation coefficient of 0.8. The failure region is shaded. When the failure modes are assumed to be independent, the joint PDF is equal to the product of two marginal PDFs of limit states, whose corresponding samples are shown in Fig. 3(b). The numbers of samples in the failure region of G_1, in the failure region of G_2, in the region of intersection and in the region of union are shown in Table 1. The numbers reflect the true probabilities and sampling errors due to the finite number of samples (the standard error in each number in the table is approximately equal to its square root).

Table 1. The number of samples in Fig. 3 (numbers in parenthesis are the numbers expected from the exact probabilities)

# of samples	Considering dependence	Ignoring dependence

$G_1 < 0$	1182 (1151)	1126 (1151)
$G_2 < 0$	1153 (1151)	1198 (1151)
$G_1 < 0$ and $G_2 < 0$	679 (665)	138 (132)
$G_1 < 0$ or $G_2 < 0$	1656 (1637)	2186 (2170)

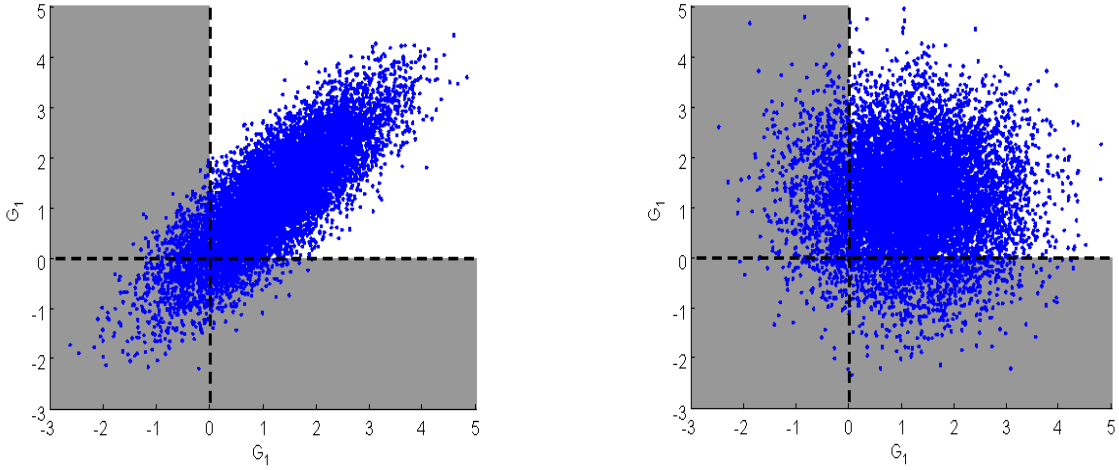

(a) Scatter plot considering dependence

$$\begin{bmatrix} X_1 \\ X_2 \end{bmatrix} \sim N\left(\begin{bmatrix} 1.2 \\ 1.2 \end{bmatrix}, \begin{bmatrix} 1 & 0.8 \\ 0.8 & 1 \end{bmatrix} \right)$$

(b) Scatter plot ignoring dependence

$X_1 \sim N(1.2,1)$ and $X_2 \sim N(1.2,1)$

Figure 3: Difference between intersection probabilities with and without considering dependence

The percent error due to ignoring dependence is calculated as

$$\text{Error} = \left| \frac{P_{f\,sys}^{idp}}{P_{f\,sys}} - 1 \right| \times 100\ (\%) \tag{9}$$

where $P_{f\,sys}$ is the system PF with dependence considered, while $P_{f\,sys}^{idp}$ is the probability assuming independence. The reliability index $\beta = -\Phi^{-1}(P_f)$ is another widely used measure, where $\Phi^{-1}(\bullet)$ is the inverse cumulative distribution function (CDF) of standard normal distribution. The error in terms of reliability index is expressed as

$$\text{Error} = \left| \frac{\beta_{sys}^{idp}}{\beta_{sys}} - 1 \right| \times 100 = \left| \frac{-\Phi^{-1}\left(P_{f\,sys}^{idp}\right)}{-\Phi^{-1}\left(P_{f\,sys}\right)} - 1 \right| \times 100\ (\%) \tag{10}$$

where β_{sys}^{idp} is reliability index ignoring dependence and β_{sys} is the reliability index with dependence considered.

B. The Effect of the Magnitude of System PF and the Strength of Dependence on Error

The effect of the magnitude of system PF and the strength of dependence given in terms of the linear correlation coefficient ρ on the error is examined for a hypothetical system with two failure modes with a bivariate normal distribution (BVN) joint PDF. By changing parameters of BVN, the effect of the level of PF and ρ on the error is studied.

Both failure modes are first assumed to have the same marginal PFs; that is, both have the same PF. The effect of different marginal PFs will be discussed later. The exact system PF is calculated from Eq. (5), while the system PF ignoring dependence is calculated from Eq. (6).

Since BVN is the joint PDF of limit states, marginal distributions are normal. The mean and standard deviation of the marginal distributions are set to z and 1, respectively. By changing the mean and the correlation coefficient, the magnitude of system PF and the strength of dependence are varied. The joint PDF of limit states and parameters are defined as

$$\begin{bmatrix} G_1 \\ G_2 \end{bmatrix} \sim N_2\left(\begin{bmatrix} z \\ z \end{bmatrix}, \begin{bmatrix} 1 & \rho \\ \rho & 1 \end{bmatrix}\right) \tag{11}$$

where $N_2(\bullet,\bullet)$ is BVN of G_1 and G_2. Since the failure is associated with negative values of limit states, the intersection probability of the two failures is obtained with cumulative distribution function (CDF) of the BVN. The error is calculated with Eqs. (9) and (10). The strength of dependence is usually categorized from very weak to very strong in terms of the linear correlation coefficient, ρ [21]. The strength of dependence is categorized to moderate, strong and very strong for $0.4 \le \rho \le 0.7$, $0.7 \le \rho \le 0.9$, and $0.9 \le \rho \le 1$, respectively. The error is calculated for strong correlation (0.7-0.9) in terms of the system PF with the range of 10^{-1} to 10^{-6}.

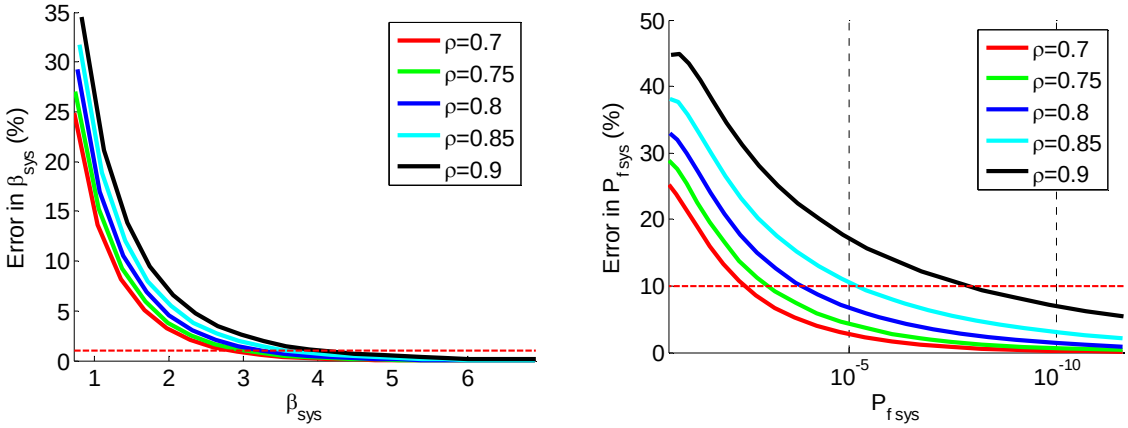

(a) Error vs reliability index (BVN) (b) Error vs PF (BVN)

Figure 4: The variation of error with the level of system PF for bivariate normal distribution with equal failure probabilities for the two modes

Table 2. Effect of linear correlation coefficient on minimum reliability index and maximum PF for the target errors due to ignoring dependence with two failure modes defined with BVN.

Reliability measure	Target error	ρ =0.7	ρ =0.75	ρ =0.8	ρ =0.85	ρ =0.9
	5%	1.68	1.79	1.93	2.10	2.31
	1%	2.82	3.03	3.28	3.60	4.04
	10%	3.4×10^{-3}	9.4×10^{-4}	1.4×10^{-4}	6.4×10^{-6}	1.6×10^{-8}
	5%	1.7×10^{-4}	2.4×10^{-5}	1.4×10^{-6}	1.1×10^{-8}	1.5×10^{-11}

The errors in reliability index and PF due to ignoring dependence are shown in Fig. 4 for different linear correlation coefficients. The errors in reliability index and PF decrease as system reliability index increases regardless the level of linear correlation coefficient. In Table 2, even with strong correlation between failure modes, ρ=0.8, the error in PF is less than 10% for the PF level less than 10^{-4}, and the error in reliability index is lower than 1% for the level of reliability index lower than 3.28. The observations imply that the interaction between failure modes becomes weak when PF is small.

One can see from Table 2 and Fig. 4 that the error in reliability index is much smaller than the error in PF. At this point, it is appropriate to note that at low probabilities of failure, small errors in input distributions may lead to small errors in reliability index but large errors in PF. Therefore, striving for very accurate small PF is out of reach anyhow. For example, distributions of failure stresses are typically based on samples of 100 tests or less. The standard error of a standard deviation of a normal distribution based on a sample of 100 is 7%. At a PF of 10^{-4}, this 7% error would lead to approximately 7% error in reliability index, but more than 50% error in PF.

C. The Effect of the Degree of Dependence in the Tail on Error

One way of measuring the dependence in the tail region is the shape of distribution. As shown in Fig. 3, independent distributions have circular-shaped contour at the failed tail region, while dependent distributions have a sharp contour in this region. For independent modes with a low PF, the low-left region of the contour is locally circular. On the other hand, if we had a distribution that is sharp in that region, as illustrated in Fig. 5(b), it indicates

that the tail dependence between the two failure modes is strong. The linear correlation coefficient is not enough to evaluate the level of tail dependence because the BVN shown in Fig. 5(a) has weaker tail dependence than the other distribution shown in Fig. 5(b) while they have the same correlation coefficient of 0.8.

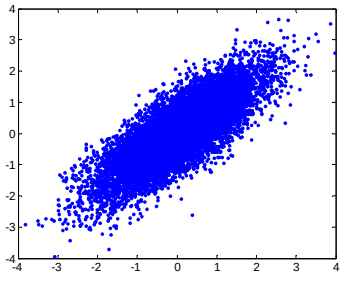

(a) ρ=0.8 (BVN)

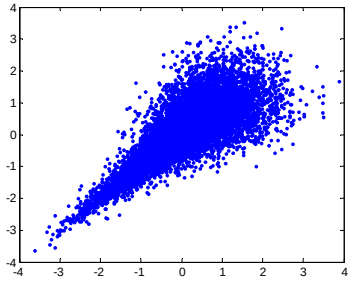

(b) ρ=0.8 (strong tail dependence)

Figure 5: Randomly generated 10,000 samples having different tail shapes with a linear correlation coefficient of 0.8

For distributions with strong tail dependence, we may expect that the error in PF decrease slowly, or will not decrease with decreasing PF. Thus, measuring the degree of tail dependence is important, for which we rely on a statistical measure, denoted by L [22], for the lower tails of two distributions. The L function is the ratio between probability of intersection and marginal probability. When independence assumption is applied to the PF, it is the ratio between the probability of double failure and the probability of the first mode of failure (or the second since they are the same). More formally, the ratio is defined as a function of marginal PF as.

$$L(z)=\Pr\left(\left\{G_1<F_{G_1}^{-1}(z)\right\}\cap\left\{G_2<F_{G_2}^{-1}(z)\right\}\right)/z \tag{12}$$

where z is the marginal probability, and $F_{G_1}^{-1}(z)$ is the inverse CDF of G_1 for given probability z.

This ratio is relevant to our case because the system PF is the sum of the two marginal probabilities of failure minus the probability of intersection (see Eq. 5). With the assumption of independence, the L function becomes z because the probability of the intersection is the square of the marginal probability. The error is then about a half of the difference between L and z.

Figure 6(a) shows the degree of dependence in the tail of BVN as a function of marginal probability and the correlation coefficient. When two limit states are independent, ρ=0, the probability of the intersection is the square of marginal probability, and the ratio is nothing but the marginal probability; i.e., L(z) = z. One can read an approximate error for different levels of system PF from the figure. For example, when z=10^{-5}, the system PF is approximately 2x10^{-5}, and for ρ =0.8, we see that L=0.14, which estimates about a 7% error in PF.

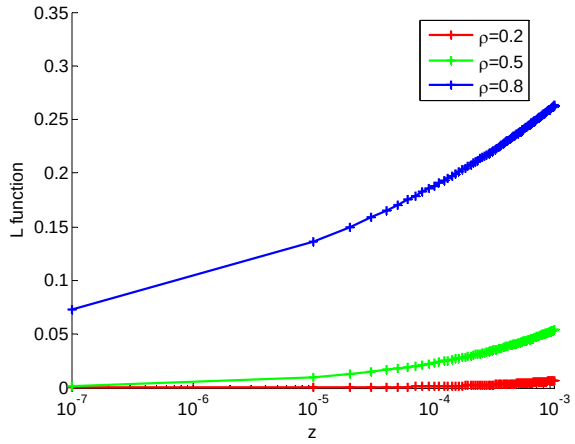

(a) L function for different values of the strength of dependence (BVN)

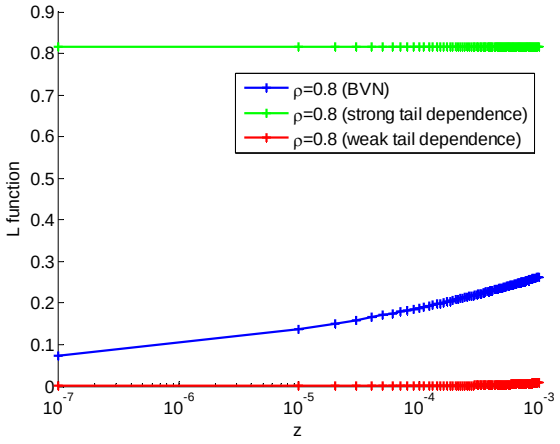

(b) L function with respect to the shape of joint PDF

Figure 6: Curves of L function with respect to the strength of dependence and tail shape of joint PDF. (Asymptotic value of $L(z)$ for $z \rightarrow +0$ is 0)

Figure 6(b) shows curves of L for three different strengths of tail dependence for a high same correlation coefficient of 0.8.The red L function curve in Fig. 6(b), a weak tail dependence case, converges faster than that of BVN. The error of neglecting dependence is smaller than that of BVN and the error becomes negligible even for a relatively large system PF. However, the green L function curve in Fig. 6(b), a strong tail dependence case, does not decrease; error remains the same even for a very small system PF. The behavior of L shows that the degree of dependence is very strong even in the extreme tail that there is almost no change in L.

Figure 7(a) shows the variation of error as a function of the level of system PF for different tail dependences. For a weak tail dependence, even with a strong correlation coefficient, ρ=0.8, the error in PF is less than 10% for the PF level less than 5×10^{-2}. On the other hand, for a strong tail dependence, the error stays high even for a low PF. On the other hand, in terms of the reliability index in Fig. 7(b), even a strong tail dependence does not change the trend of low errors for high values of reliability index (low values of the PF).

Table 3 presents the magnitudes of maximum system PF and minimum reliability index for different target errors. For example, for the weak tail dependence, in terms of reliability index, there is only 1% error when system reliability index is 1.98.

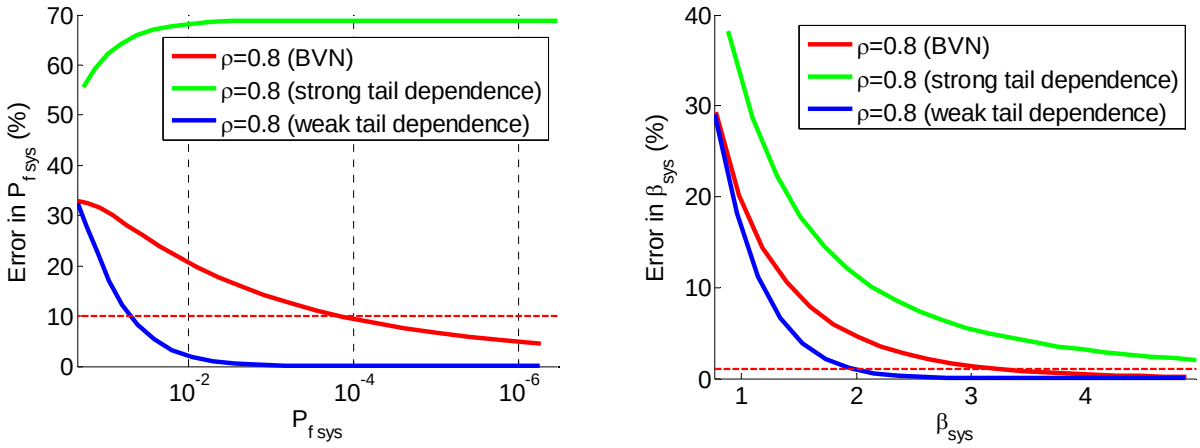

(a) Error vs PF (b) Error vs reliability index

Figure 7: The magnitude of error with respect to the strength of tail dependence

Table 3. Minimum reliability index and maximum PF needed for the target errors with respect to the strength of tail dependence for given magnitudes of error

Reliability measure	Target error	ρ =0.8 (BVN)	ρ =0.8 (strong tail dependence)	ρ =0.8 (weak tail dependence)
	5%	1.93	3.13	1.44
	1%	3.28	6.92	1.98
	10%	1.4×10^{-4}	N/A	5.0×10^{-2}
	5%	1.3×10^{-6}	N/A	2.5×10^{-2}

From Table 3, we can observe that the error in system PF will not reduce, or reduce more slowly with decreasing PF, while the error in reliability index will still reduce even for distributions with strong tail dependence. A positive side is that the error in reliability index decreases even with strong tail dependence as shown in Fig. 7(b).

We use the L function as a measure of the degree of tail dependence herein. Another common approach to measure the degree of tail dependence is to estimate TDC [23]. The limit of L is referred to as tail dependence coefficient (TDC) that represents the strength of tail dependence [20].

$$\text{TDC} = \lim_{z \to +0} L(z) \tag{13}$$

L for BVN converges to zero as z approaches zero that error due to ignoring dependence decreases as system PF decreases. However, distributions with strong tail dependence have non zero TDC. Unfortunately, accurate TDC estimation to determine the degree of tail dependence requires more than 1,000 samples, which may always not be feasible [23].

IV. Reliability based Design with Two Failure Modes

Reliability based design optimization (RBDO) is performed to demonstrate further the effect of ignoring dependence for a structure which is required to be highly reliable. The previous truss structure in Fig. 1 is used for RBDO. The optimization formulation is given as

$$\begin{aligned} &\text{Minimize: } Mass = A_1 + A_2 \\ &\text{Subject to: } \beta_{allow} < -\Phi^{-1}\left(P_{f,sys}\right) \\ &P_{f,sys} = \Pr\left(\{G_1 < 0\} \cup \{G_2 < 0\}\right) \end{aligned} \tag{14}$$

where A_1 and A_2 are design variables. FORM is used to evaluate marginal PFs during design optimization iterations and the system PF is calculated by assuming independence. Since the limit states are linear functions of random variables, FORM provides exact marginal PFs of two failure modes, the failure modes are statistically dependent. Table 4 shows the uncertainty information of input variables.

Table 4. Input variables

Uncertainty variables		Deterministic variables	
Vertical force (v)	N(30000, 4500) KN	Angle (α)	45 (degree)
Horizontal force (h)	N(7000, 350) N	Height (l)	1 m
Ultimate strength (σ_u)	N(250,12.5) MPa		

Figure 8 (a) shows the weight and system reliability index in terms of design variables. The solid lines with label (equivalent reliability index) are exact contour lines for system reliability index and the dashed lines are corresponding contour lines with independence assumption. The discrepancy between the solid line and the dashed lines represents the error, and the difference in weight due to the error is defined as a weight penalty. For the same allowed system reliability index, some part does not have discrepancy between two constraint lines since one failure mode is dominant so that there is no error in calculating the system reliability index. The filled 2D contour is weight, where light gray represents heavy weight and dark gray represents light weight. Optimum solution provides minimum weight while the system reliability index constraint is not violated. The star marker is the exact optimum solution and the circle marker is the optimum solution ignoring dependence for the target system reliability of β_{allow} = 3.5 (PF_{allow}=0.00023). The red line contains minimum weight designs satisfying different reliability constraints. For example, the minimum weight design for the reliability constraint of β_{allow} = 2.5 (PF_{allow}=0.0062) is at the crossing point between the β_{allow} = 2.5 constraint line and the red line.

As shown in Fig. 7(b), the magnitude of error is inversely proportional to the system reliability index. For the target system reliability of β_{allow} = 3.5, the error is very small, while the errors for β_{allow} = 1.5 (PF_{allow}=0.067) and β_{allow} = 2 (PF_{allow}=0.023) are clearly visible.

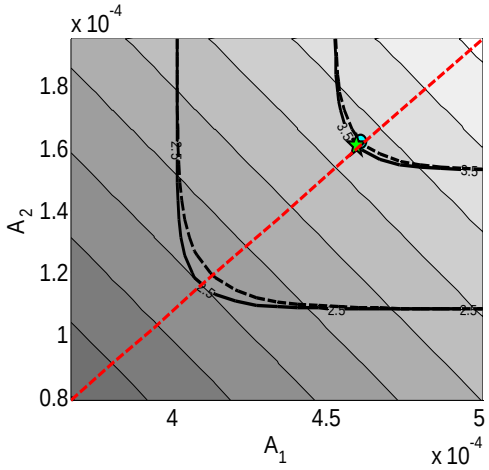

(a) Weight (bright and dark color represent heavy and light weight, respectively) and constraint lines with respect to the magnitude of allowable reliability index

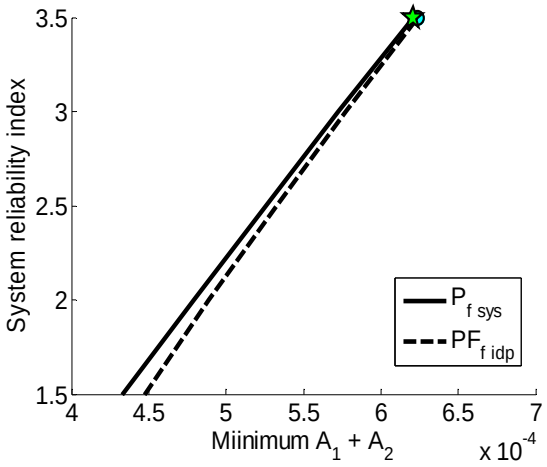

(b) Minimum A_1+A_2 and corresponding reliability index

Figure 8: Visualization of probabilistic optimization results

Figure 8 (b) shows minimum weight for given allowed system reliability indices. The star and circle markers are the exact optimum solution and the optimum solution with independence assumption, respectively. There is 3.1% weight penalty for β_{allow} = 1.5 and the weight penalty is reduced to 0.5% for β_{allow} = 3.5. Note, however, that this additional weight is accompanied by improved safety. For example, the safety improvement by the error in system PF calculation for β_{allow} = 3.5 is 11%. The exact optimum design with exact PF calculation (the star marker) is 0.000233 while the optimum design with ignoring dependence is 0.000208.

For the allowable reliability index of 3.5, at the optimal design point, the correlation coefficient between the two failure modes is 0.8 and the ratio between marginal probabilities of failure is 1.12 (P_1=0.00014 and P_2=0.00012).

The strong correlation is due to the fact that randomness in the loads and strength affects the two failure modes in a similar way. However, that dependence does not mean that design improvement in one failure will affect the other failure. For this optimization problem, A_1 will affect only the reliability of element 1 and A_2 will affect only the reliability of element 2.

V. The Effect of Errors in Input Distributions

From the previous examples, error due to ignoring dependence is less than 10% for small system PF when tail dependence between two failure modes is not strong. For strong tail dependence, errors may be as much as 70%, and they do not decrease as PF decreases. However, for small PF, expecting small error in system PF calculation is unrealistic due to unavoidable small errors in distributions defining input uncertainties. In real practice, input uncertainties are usually determined from a finite number of samples incurring small sampling errors. As noted before, and as will be illustrated below for the truss example, small sampling errors cause large relative errors in the calculation of small probabilities of failure.

For the previous two bar truss example, there are four uncertain input variables, the uncertainties in the horizontal and vertical loads, in the ultimate strengths of two bars. In this study, we used the distributions in Table 4 as the true input distributions of the truss example. We assume that there is no error in selecting distribution types and load distributions and only consider errors in the mean and standard deviation of the ultimate strength due to sampling errors. We examined the effect of errors in input distributions on errors in system PF by comparing system PF of one design using the true input distributions and system PF of the same design but using input distributions with errors as shown in Table 5. To see the pure effect of errors in input distribution, exact system PFs were evaluated.

Table 5. Input variables with errors

Uncertainty variables		Deterministic variables	
Vertical force (v)	N(30000, 4500) KN	Angle (α)	45 (degree)
Horizontal force (h)	N(7000, 350) N	Height (l)	1 m

Ultimate strength (σ_u)	$N(\mu_{test},\sigma_{test})$ MPa

The parameters of the ultimate strength are estimated using coupon tests. Since the ultimate strength follows a normal distribution with the mean of 250 MPa and the standard deviation of 12.5 MPa, the sample mean and sample standard deviation of the ultimate strength are expressed in terms of the number of samples. When the number of samples is n then the sample mean and standard deviations are expressed as

$$\mu_{test} \sim N\left(250, \frac{12.5}{\sqrt{n}}\right) \tag{15}$$

$$\frac{\sigma_{test}^{\ 2}(n-1)}{12.5^2} \sim \chi^2(n-1) \tag{16}$$

where χ^2 is a chi squared distribution with the degree of freedom n-1.

After errors in the load distributions and the sample mean and sample standard deviation are generated using Eqs. (15) and (16), the corresponding system PFs, errors in system PF and errors in system reliability index are calculated. One randomly generated errors and sample parameters give one error in PF calculation. For example, from N=100,000 randomly generated errors, test means and test standard deviations, we can collect N =100,000 errors in system PF calculation. The error in PF and the error in reliability index due to errors in input distributions are calculated as

$$e_i = \left(\frac{PF_i}{PF_{true}} - 1\right) \times 100 \quad i = 1,2,...,N \tag{17}$$

$$e_i = \left(\frac{-\Phi^{-1}(PF_i)}{-\Phi^{-1}PF_{true}} - 1\right) \times 100 \quad i = 1,2,...,N \tag{18}$$

where i is a sample index.

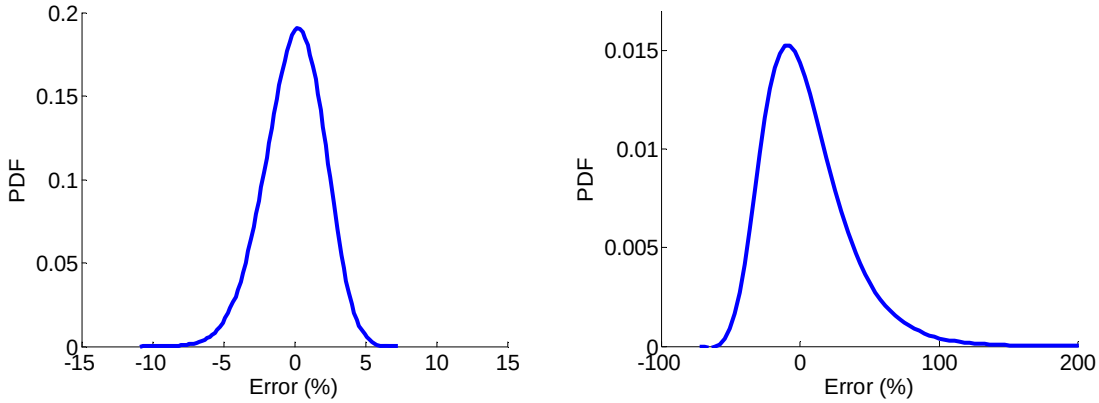

Distribution of error in reliability index Distribution of error in PF

Figure 9: Error distributions for the errors in input distribution parameters.

Figure 9 shows that the error distributions due to errors in the input parameters for the optimum design satisfying the reliability constraint β_{allow} = 3.5 (PF_{allow}=0.00023). The error in reliability index and the error in PF are shown. At the optimum design, the true system PF is $\Phi(-3.5)$ for the true input parameters. We generated 100,000 errors in the parameters, calculate the corresponding errors in system PF calculation and plotted as a PDF form. The error in reliability index is much smaller than that in PF. Also we can see that the effect of errors in the input parameters leads huge error in system PF calculation.

These errors are due to multiple sources: errors in sample mean and sample standard deviation of the ultimate strength. The contribution of individual sources is given in Table 6. Since errors are defined with distributions we employ the root mean square error (RMSE) and the mean absolute error (MAE) to summarize the effects of uncertainties. The measures are expressed as

$$RMSE = \sqrt{\frac{1}{N}\sum_{i=1}^{N} e_i^2} \tag{19}$$

$$\text{MAE}=\frac{1}{N}\sum_{i=1}^{N}|e_i| \tag{20}$$

Table 6 shows the effect of errors in terms of the measurements for different uncertainty sources and the number of tests. For example, the results of "Error in the mean of the ultimate strength" are only because of the error in the mean of the ultimate strength. We can see that the error in sample standard deviation is the most influential factor and the error in sample mean is second most influential factor. Errors in the load distribution parameters are not influential as much as the errors in the ultimate strength parameters. From the change of the error measures in terms of the number of tests, the efficiency of increasing the number of tests decreases as the number increases. For the increase of the number of tests from 30 to 50, the change of RMSE of error in PF is 5.4 but for the changed of the number of tests from 50 to 100 gives very similar improvement. Figure 10 also provides the same observation.

Table 6. The effect of uncertainty source combinations in terms of RMSE and MAE

Considered uncertainty sources	# of tests	Error in PF		Error in reliability index	
		RMSE	MAE	RMSE	MAE
	30	23.0	17.8	1.6	1.3
	50	17.6	13.6	1.2	1.0
	100	12.3	9.7	0.9	0.7
	30	30.3	22.1	2.0	1.6
	50	22.5	16.9	1.5	1.2
	100	14.9	11.6	1.0	0.8
	30	41.0	29.8	2.6	2.1
	50	30.2	22.7	2.0	1.6
	100	20.5	15.8	1.4	1.1

Figure 10 shows that the effect of errors in input distributions in terms of RMSE and MAE of error in system PF for the system PF range of 10^{-4} to 10^{-6}. RMSE becomes larger than 70% and MAE becomes comparable to 70%. That is the error of 70% in system PF calculation due to strong tail dependence is more than comparable to the error due to errors in the input distributions.

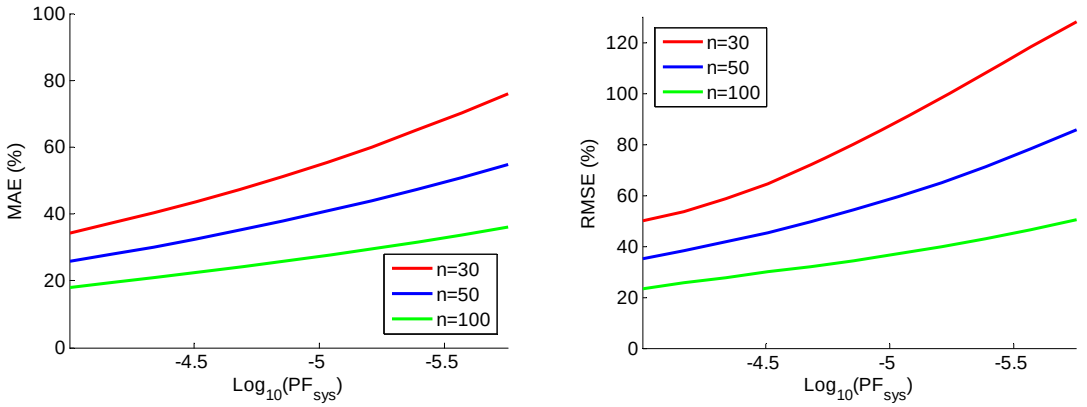

Figure 10: Curves for RMSE and MAE in terms of error in PF.

VI. Concluding Remarks

In this paper, the effect of ignoring dependence between failure modes was studied. The effects of tail dependence and the ratio between marginal PFs were found to be significant. For low probabilities of failure, we can conclude that: 1) for errors in system reliability index, we can neglect dependence even for strong tail dependence and 2) for errors in system PF, we can neglect dependence when the ratio of marginal PFs is high or tail dependence is not very strong. 3) for errors in system PF, errors due to errors in input distribution parameters are also comparable to errors due to ignoring strong tail dependence.

To demonstrate the effect of ignoring dependence, we started with two failure modes obeying the bivariate normal (BVN) distribution. For the BVN with strong dependence with a correlation coefficient of ρ = 0.8, there is 1% error in the system reliability index at 3.28, and there is 10% error in system PF at 10-4.

For other distributions, the decay of errors with increasing reliability index depends on a parameter called tail dependence. For strong tail dependence between failure modes, such as the Clayton copula, the errors in system PF do not decay even for a low system PF. However, the errors in system reliability index still decay fast for high reliability index. Possibly, small errors in large values of reliability index are acceptable even if the relative errors in PF are high. This is because similar large errors in PF are inevitable due to small errors in input distributions.

Appendix

A. Copula Models

The previous sections presented results for BVN and generic strong and weak dependence. In this section, a more general approach will be taken to describe correlation types of distributions. Joint distributions are often modeled by using copulas, and three copulas in Fig. A1 are the copulas used to explain the effect of tail dependence and the corresponding error in neglecting the dependence in Fig. 7. The strong tail dependence is modeled the Clayton copula and the weak tail dependence is modeled with the Frank copula. BVN is defined with the Gaussian copula with normal marginal distributions.

The word 'copula' is a Latin noun which means "a link". The word was employed in a statistical term by Sklar (1959) in the theorem describing the functions that join marginal CDF to form a joint CDF [18]. In this context, copula is a function that links a joint CDF to its marginal CDFs [19,20,21]. Copula is a joint CDF whose one-dimensional margins are uniform in the interval (0,1). Copula is an important concept for modeling a joint CDF that includes dependence.

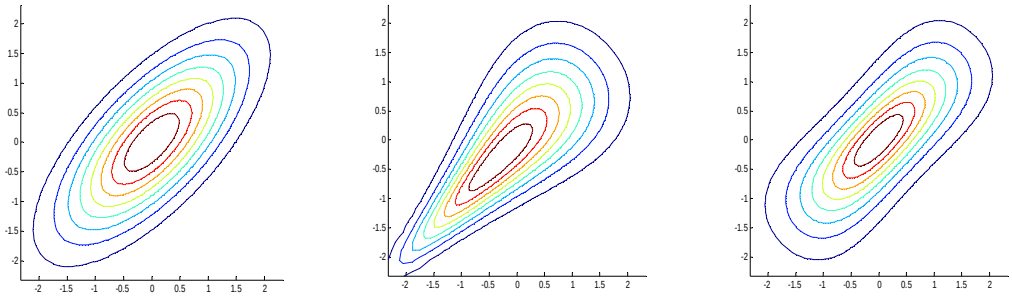

(a) Gaussian copula (b) Clayton copula (c) Frank copula

Figure A1: Four joint PDF shapes with commonly used copulas with two standard normal marginal distributions with a linear correlation coefficient of 0.7

Let $\mathbf{Y}=\{Y_1,Y_2,...,Y_n\}^T$ be a vector of n-dimensional random variables, which are defined with marginal CDFs, $F_{Y_i}(y_i)$. The probability of intersection is a function of dependence. The probability of intersection of n-dimensional random variables is also called a joint CDF that is defined as

$$F_{Y_1,...Y_n}(y_1,...,y_n)=\Pr(Y_1\le y_1,...,Y_n\le y_n) \tag{A1}$$

Copula functions defines the joint CDF with marginal CDFs

$$F_{Y_1,...Y_n}(y_1,...,y_n)=C\left(F_{Y_1}(y_1),...,F_{Y_n}(y_n)\right) \tag{A2}$$

where C is a copula function. Note that copula functions are independent to marginal CDFs and all arguments of copula function have a domain of [0, 1]. Also, due to the property of multivariate CDF, the output of the copula function also has a domain of [0, 1].

Figure A2 shows L function for the copulas shown in Fig. A1. As expected, the copula with a sharp tail, Clayton, has a very strong tail dependence. Gaussian copula has stronger tail dependence than Gumbel and Clayton copulas.

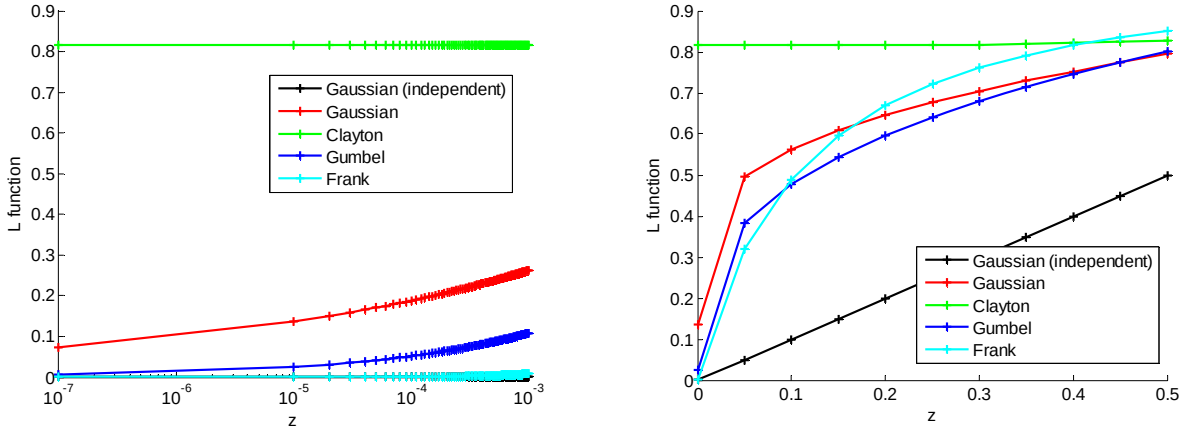

(a) L function in extreme tail region (b) L function for macroscopic scale

Figure A2: L functions for different copulas

It is noteworthy that the type of marginal distributions is immaterial as far as the error due to ignoring dependence is concerned. The error is a function of the magnitude of system PF and the type of copula. For example, if the marginal distributions are lognormal and the copula defining the joint distribution is Gaussian, then the error will be the same as in the case of BVN.

B. The Effect of Ignoring Dependence for Different Copulas

In the previous section, the error due to ignoring dependence for BVN, which is defined with a Gaussian copula, is shown as a function of the magnitude of system PF and the correlation coefficient. In this section, the errors with different dependence models are defined with Clayton, Gumbel and Frank copulas. Since the type of marginal distributions is immaterial to the error, the normal distributions are used as marginal CDFs. Then, the errors are calculated in terms of system PF and reliability index. The system PF shown in Eq. (5) is rewritten using copula as

$$P_{f,sys} = F(0,z,1) + F(0,z,1) - C\left(F(0,z,1), F(0,z,1), \theta\right)$$
$$\beta_{sys} = -\Phi^{-1}\left(P_{f,sys}\right) \tag{B1}$$

The magnitude of PF and the strength of dependence are controlled by changing z and θ. PF ignoring dependence is expressed as

$$P_{f,ind} = F_{G_1}(0,z,1) + F_{G_2}(0,z,1) - F_{G_1}(0,z,1) F_{G_2}(0,z,1) \tag{B2}$$

The errors in Eqs. (9) and (10) are shown in Fig. B1 for a range of correlation coefficients. It is observed that the error in reliability index decreases as system reliability increases even for strong tail dependence. In the case of system PF, however, the error does not decrease for the Clayton copula, but the error decreases for the other two copulas.

Although the Kendall's tau is used to define the level of dependence, the corresponding linear correlation coefficient is shown for the purpose of consistency. Since there is no universal way to convert Kendall's tau to the linear correlation coefficient, we generate 10,000 samples with a given level of Kendall's tau, from which the corresponding linear correlation coefficient is calculated. This process is repeated for different Kendall's tau to find the specific value of linear coefficient. It is noted that different copulas yield different values of linear correlation coefficients for the same value of Kendall's tau. For example, Kendall's tau of 0.63 with the Clayton copula and standard normal marginal distributions has the strength of dependence 0.8 in terms of the correlation coefficient.

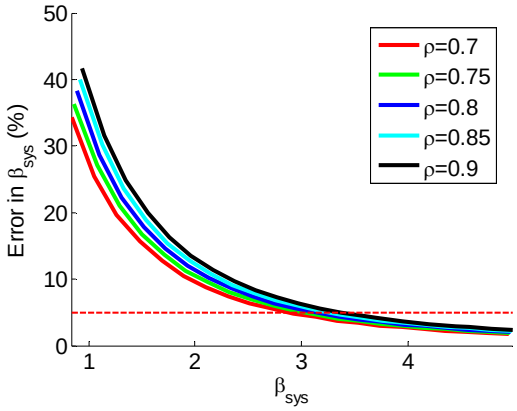

(a) Error vs reliability index (Clayton)

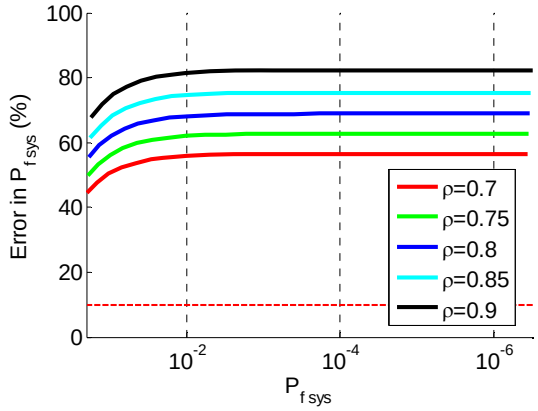

(b) Error vs log PF (Clayton)

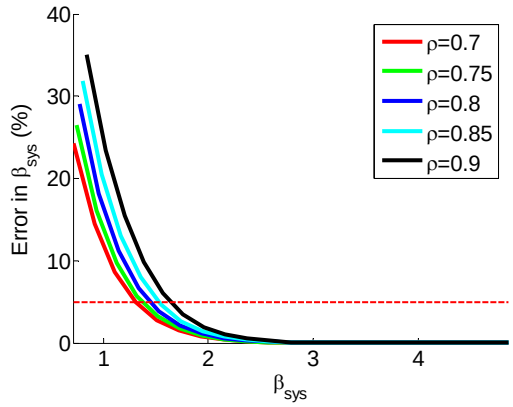

(c) Error vs reliability index (Frank)

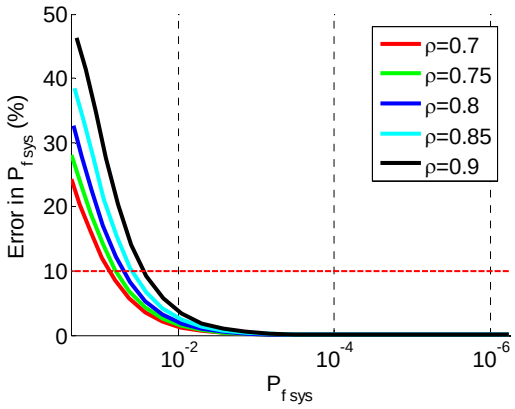

(d) Error vs log PF (Frank)

Figure B1: The relative error in reliability index (left figures) and PFs (right figures) versus system PF

Table 4 presents the magnitudes of minimum system reliability indices for 5% and 1% target errors. From Fig. B1 and Table B1, we see that, as expected, for the Frank copula, which has weak tail dependence, the errors in the reliability index decay fast for high reliability index. However, even for the Clayton copula with a strong tail dependence, the error reduces relatively fast. Error in the reliability index converges to zero as the reliability index increases. In Table B2, the magnitudes of maximum system PFs for 10% and 5% errors are shown. The error in PF with Frank copula decrease as reliability indices increase since they have a weak tail dependence. For Frank copula, the error becomes less than 5% at the level of 10^{-3} even at the very large correlation coefficient of ρ = 0.9. For the Clayton copula model, on the other hand, the error in PF increases as reliability increases due to its strong tail dependence.

Table B1. Minimum reliability index for 5% and 1% target errors (in reliability index) versus the strength of dependence measured by the linear correlation coefficient

Copula	Target error \ ρ	ρ =0.7	ρ =0.75	ρ =0.8	ρ =0.85	ρ =0.9
	5%	2.88	3.01	3.14	3.26	3.38
	1%	6.50	6.72	6.92	7.10	7.27
	5%	1.30	1.37	1.44	1.53	1.63
	1%	1.86	1.92	1.98	2.06	2.17

Table B2. Maximum system PF for 10% and 5% target errors in PF (not error in logarithm of PF) with respect to the strength of dependence measured by the linear correlation coefficient

Copula	Target error	ρ =0.7	ρ =0.75	ρ =0.8	ρ =0.85	ρ =0.9
Clayton				N/A[1]		
	10%	7.7×10^{-2}	6.3×10^{-2}	5.0×10^{-2}	3.9×10^{-2}	2.7×10^{-2}
	5%	7.3×10^{-3}	6.0×10^{-3}	4.9×10^{-3}	3.8×10^{-3}	2.7×10^{-3}

[1] Error for Clayton is always larger than 10% for the level of PF less than 0.01

Acknowledgments

Authors would like to thank the Air Force Research Laboratory for supporting this work under the contract 84796.

References

[1]J. Li, J. Chen, and W. Fan. The Equivalent Extreme-value Event and Evaluation of the Structural System Reliability, Structural Safety 2007;29(2):112-13.

[2]R. E. Melchers. Important Sampling in Structural Systems. Structural Safety 1989;6: 3-10.

[3]Melchers R. E. Structural Reliability Analysis and Prediction. New York: Wiley; 1999.

[4]A. Dey, and S. Mahadevan, Ductile Structural System Reliability Analysis using Adoptive Importance Sampling. Structural Safety 1998; 20:137-154.

[5]Zheng Y., Das P. K. Improved response surface method and its application to stiffened plate reliability analysis. Engineering Structures 2000;22:544-551.

[6]Ba-abbad, M. A. Nikolaidis, E., and Kapania, R. K., New Approach for System Reliability-Based Design Optimization. AIAA Journal 2003; 44(5): 1087-1096.

[7]Haldar, A., and Mahadevan, S. Probability, Reliability and Statistical Methods in Engineering Design. New York: John Wiley & Sons; 2000.

[8]M. Hohenbichler and R. Rackwitz First-Order Concepts in System Reliability. Structural Safety 1983;1:177-188.

[9]Vanmarcke EH. Matrix form formulation of reliability analysis and reliability-based design. Comput Struct 1973;3(4):757–70.

[10]Ang AH-S, Abdelnour J, Chaker AA. Analysis of activity networks under uncertainty. J Eng Mech Div ASCE 1975;101(EM4):373–87.

[11]Schmidt, R. Tail dependence for elliptically contoured distributions. Math. Methods Oper. Res. 2002;55:301–327.

[12]Ditlevsen O. Narrow reliability bounds for structural systems. J Struct Mech 1979;7:453–72.

[13]Eishakoff, Issac. Safety Factors and Reliability; Friends or Foes? Springer; 2004.

[14]D.M. Neal, W.T. Matthews, M.G. Vangel and T. Rudalevige. A Sensitivity Analysis on Component Reliability from Fatigue Life Computations; U.S. Army Materials Technology Laboratory, Report No. MTL TR 92-5; 1992.

[15]Y. Noh. Input model uncertainty and reliability-based design optimization with associated confidence level, Ph D. dissertation, Department of Mechanical Engineering, University of Iowa, 2009.

[16]Y. Noh, K. K. Choi, and I. Lee. Identification of marginal and joint CDFs using Bayesian method for RBDO, Structural and Multidisciplinary Optimization 2010; 40: 35-51.

[17]C. Park, N. H. Kim, R. T. Haftka. The Effect of Ignoring Dependence between Failure Modes on Evaluating Structural Reliability, *10th World Congresses of Structural and Multidisciplinary Optimization*, Orlando, USA, May *19-24*, 2013.

[18]Sklar. A. Fonctions de répartition à n dimensions et leurs marges. *Publ. Inst. Statist. Univ. Paris* 1959;8: 229–231.

[19]Nelson R.B. An Introduction to Copula, Springer. New York: Springer; 1999.

[20]H. Joe, Multivariate Models and Dependence Concepts. Vol. 73: CRC Press; 1997.

[21]P. Georges, A-G. Lamy, E. Nicholas, G. Quibel, T. Roncalli. Multivariate survival modeling: a unified approach with copulas. Groupe de Recherche Opérationnelle Crédit Lyonnais France; 2001.

[22]Venter, G.G. Tails of copulas. In *Proceedings of the Casualty Actuarial society* 2002;89: 68–113.

[23]G. Frahm , M. Junker, and R. Schmidt. Estimating the tail-dependence coefficient: Properties and pitfalls, Insurance: Mathematics and Economics 2006;37:80-100.

[24]J. Li, J. Chen, and W. Fan. The Equivalent Extreme-value Event and Evaluation of the Structural System Reliability, Structural Safety 2007;29(2):112-13.